Biochimica et Biophysica Acta 1832 (2013) 347–354

Contents lists available at SciVerse ScienceDirect

Biochimica et Biophysica Acta

journal homepage: www.elsevier.com/locate/bbadis

Matrix Metalloproteinase 1 promotes tumor formation and lung metastasis in an intratibial injection osteosarcoma mouse model

Knut Husmann *, Matthias J.E. Arlt, Roman Muff, Bettina Langsam, Josefine Bertz, Walter Born, Bruno Fuchs

Laboratory for Orthopedic Research, Department of Orthopedics, Balgrist University Hospital, University of Zurich, Zurich, Switzerland

ARTICLE INFO

Article history:
Received 30 July 2012
Received in revised form 6 November 2012
Accepted 9 November 2012
Available online 27 November 2012

Keywords:
Osteosarcoma
Metastasis
MMP-1
In vivo
Intratibial mouse model

ABSTRACT

Proteolytic degradation of the extracellular matrix (ECM) is an important process during tumor invasion. Matrix Metalloproteinase 1 (MMP-1) is one of the proteases that degrade collagen type I, a major component of bone ECM. In the present study, the biological relevance of MMP-1 in osteosarcoma (OS) tumor growth and metastasis was investigated in vitro and in vivo. Human OS cells in primary culture expressed MMP-1 encoding mRNA at considerably higher levels than normal human bone cells. In addition, MMP-1 mRNA and protein expression in the highly metastatic human osteosarcoma 143-B cell line was remarkably higher than in the non-metastatic parental HOS cell line. Stable shRNA-mediated downregulation of MMP-1 in 143-B cells impaired adhesion to collagen I and anchorage-independent growth, reflected by a reduced ability to grow in soft agar. Upon intratibial injection into SCID mice, 143-B cells with shRNA-downregulated MMP-1 expression formed smaller primary tumors and significantly lower numbers of lung micro- and macrometastases than control cells. Conversely, HOS cells stably overexpressing MMP-1 showed an enhanced adhesion capability to collagen I and accelerated anchorage-independent growth compared to empty vector-transduced control cells. Furthermore, and most importantly, individual MMP-1 overexpression in HOS cells enabled the formation of osteolytic primary tumors and lung metastasis while the HOS control cells did not develop any tumors or metastases after intratibial injection. The findings of the present study reveal an important role of MMP-1 in OS primary tumor and metastasis formation to the lung, the major organ of OS metastasis.

1. Introduction

Osteosarcoma (OS) is a highly malignant bone tumor mainly affecting children and young adults. Continuous progress in neo-adjuvant chemotherapy increased the 5-year survival rate of patients over the past 30 years from 20% to 70%. However, patients who present with metastases at diagnosis, predominantly in the lung, continue to have a poor 5-year survival rate of approximately 20% [1]. Consequently, the identification of novel targets for better diagnosis and more effective treatment of OS patients with metastatic disease are of great importance.

Metastasis of primary tumor cells to distant organs is a complex, multistage process that includes aberrantly regulated biological events such as uncontrolled cell proliferation, tissue remodeling, angiogenesis and invasion [2]. The colonization of tumor cells of different cancer types in distant organs requires the expression of distinct protein sets at variable time periods [3]. Proteolytic enzymes including metallo-, serine-, aspartyl-, and cysteine proteases are involved in different steps of metastasis [4,5]. These enzymes act either directly by degrading extracellular matrix (ECM) and cell surface proteins, or indirectly through the activation of cascades of proteolytic enzymes and the release of effector proteins associated with the ECM [6].

The class of matrix metalloproteinases (MMPs) comprises more than 20 extracellular zinc-dependent endopeptidases. The expression of these proteins is regulated at the level of transcription and their enzymatic activity by proteolytic activation and by selective inhibitory proteins. Almost all components of the ECM and a wide variety of non-matrix proteins are substrates of MMPs [7]. MMPs play an important role in ECM remodeling in diverse physiological processes including development, regeneration, and wound healing. They are also involved in different pathological processes such as rheumatoid arthritis, osteoarthritis, pulmonary emphysema, and cancer [8].

Matrix-metalloproteinase 1 (MMP-1), also known as collagenase-1, is nondetectable in normal tissues, but its expression is rapidly induced when tissue remodeling is needed. MMP-1 is able to cleave in vitro several components of the ECM including the collagen types I, II, III, VII, VIII and X as well as laminin, tenascin, aggrecan, and serine protease inhibitors [9]. In cancer, MMP-1 is expressed by tumor cells or by surrounding stromal fibroblasts at the site of invasion, indicating the functional relevance of the protein in this process [10]. MMP-1 has been described as a prognostic marker for different types of

* Corresponding author at: Laboratory for Orthopedic Research, Balgrist University Hospital, Forchstrasse 340, CH-8008 Zurich, Switzerland. Tel.: +41 44 386 1665; fax: +41 44 386 1669.
E-mail address: research@balgrist.ch (K. Husmann).

0925-4439/$ – see front matter © 2012 Elsevier B.V. All rights reserved.
http://dx.doi.org/10.1016/j.bbadis.2012.11.006

cancers such as melanoma, colorectal and esophageal cancer and chondrosarcoma, with an inverse correlation between survival and MMP-1 expression [11–14]. Recently, Kang et al. [15] showed that MMP-1—together with CXCR4 and IL-11—was highly overexpressed in breast cancer cells that metastasized to bone and formed osteolytic lesions in athymic nude mice.

Bone connective tissue has a functionally optimized composition. Collagen is the main organic component of the ECM in normal bone and consists predominantly of collagen type I. The protein is assembled in insoluble fibers that contribute to the structural integrity and mechanical stability of bone. Only a few proteases, including cathepsin K, MMP-1, -8, -13 and -14, are capable to cleave native fibrillar collagen type I [16]. The activity of one or several of these proteases is a prerequisite for the degradation of bone ECM, which is then completed by other proteases and allows primary tumor growth and extravasation of tumor cells to distant organs.

Increased MMP-2 (gelatinase-A) and MMP-9 (gelatinase-B) expression was identified as prognostic markers for poor outcome of OS [17–19]. However, for MMP-8 (collagenase-2) and MMP-13 (collagenase-3) a correlation between protein expression in clinical samples and patient survival was not observed [20], and, to our knowledge, the relevance of MMP-1 for the outcome of OS has so far not been investigated. In the present study, a comparison of MMP-1 expression at the transcript level in cells of normal bone and of OS cells in primary culture indicated an upregulation of MMP-1 in all OS cell specimens collected from a series of primary tumors. Based on these findings, we investigated the biological relevance of MMP-1 for primary tumor growth and metastasis in an intratibial human xenograft OS model in SCID mice. MMP-1 was knocked-down in the highly metastatic human OS cell line 143-B with robust endogenous MMP-1 expression and the proteinase was overexpressed in the parental non-metastatic HOS cell line with hardly detectable endogenous MMP-1. The results demonstrate an important malignancy promoting role of MMP-1 in experimental human OS.

2. Materials and methods

2.1. Cell lines and culture conditions

HOS, MNNG/HOS and HEK293-T cells were purchased from the American Type Culture Collection (Rockville, MD) and 143-B cells from the European Collection of Cell Cultures (Salisbury, UK). All cell lines were grown in Dulbecco's modified Eagle medium (DMEM) (4.5 g/L glucose) and Ham F12 (F12) medium (1:1) supplemented with 10% fetal calf serum (FCS) (GIBCO, Basel, Switzerland) (cell culture medium) in a humidified atmosphere of 95% air and 5% CO_2 at 37 °C. Normal human bone (NHB) and primary OS cells were isolated as described [21] and grown in cell culture medium supplemented with penicillin/streptomycin/amphotericin (PSA, 1:100, Invitrogen, Carlsbad, CA). The tissue collection for generation of primary cells was approved by the ethical committee of the Kanton of Zurich (reference number EK-10-2007).

2.2. RNA isolation and RT-PCR

Total RNA was isolated from individual cell lines with TriReagent (Sigma-Aldrich, St. Louis, MO) as described [22]. The RNA was quantified by measuring the absorption at 260 and 280 nm in a UV-spectrophotometer and RNA integrity was assessed by standard agarose gel-electrophoresis. The expression of MMP-1, MMP-8 and MMP-13 encoding mRNA was analyzed by reverse transcriptase (RT)-PCR with GAPDH as a reference gene. cDNA was synthesized from 1 μg of total RNA with the High Capacity cDNA Reverse Transcription Kit (Applied Biosystems, Foster City, CA) and the protocol recommended by the supplier. PCR reactions of 50 μl final volume contained 1× PCR buffer, 0.4 μl of the reverse transcription reaction, 1.25 U Taq polymerase (5Prime, Gaithersburg, MD), 200 μM of each dNTP, and 0.2 μM of forward and reverse primer pairs specific for the individual marker transcripts (GAPDH Forward: TGA ACG GGA AGC TCA CTG GCA TGG; GAPDH Reverse: TGG GTG TCG CTG TTG AAG TCA GAG GAG A; MMP-1 Forward: CTC GGC CAT TCT CTT GGA CTC TCC CAT T, MMP-1 Reverse: AGC ATC AAA GGT TAG CTT ACT GTC ACA CGC; MMP-8 Forward: CCT ATT TAA AGG CAA CCA ATA CTG GGC TCT; MMP-8 Reverse: TTT GGG ATA ACC TGG CTC CAT GAA TTG TCT; MMP-13 Forward: ATC CCT TGA TGC CAT TAC CAG TCT CCG A; MMP-13 Reverse: AGA TGA AGA TGA GGT CAT GAG AAG GGT GC). After initial denaturation at 94 °C for 3 min, DNA was amplified by 27 to 40 PCR-cycles (denaturation at 94 °C for 40 s, primer pair-dependent annealing at 67 °C to 69 °C for 40 s, and elongation at 72 °C for 20 s) followed by a final elongation step at 72 °C for 7 min. PCR products were analyzed by agarose gel (1.2%) electrophoresis.

2.3. Real-time PCR analysis

The cDNAs from NHB cells (4 samples) and primary OS cells (eighteen samples) were analyzed in triplicates using a Step One Plus real-time PCR instrument (Applied Biosystems). 10 ng of cDNA, the primer pairs described in the previous paragraph and the Power SYBR® Green PCR master mix (Applied Biosystems) in a volume of 10 μl per reaction were used. GAPDH was chosen as a suitable normalization control gene. Results were obtained by the comparative Ct method [23], using ΔCt (the value for individual samples was obtained by subtracting the Ct value of MMP-1 from the Ct value of GAPDH). Primary OS cells with at least two-fold higher MMP-1 mRNA expression than the normal human bone cells were defined as MMP-1 overexpressing cells.

2.4. Construction and generation of recombinant retrovirus

MMP-1 encoding cDNA was amplified by RT-PCR from total RNA isolated from 143-B cells with the following primer pair: Forward: TTG CAC TGA GAA AGA AGA CAA AGG and Reverse: TGA GAA AAT AGA CAG TTC TTC AGG. The PCR product was cloned into the pGEM®-T Easy Vector (Promega, Madison, WI) and the sequence was verified by sequencing of both strands. The MMP-1 cDNA was then subcloned into the retroviral pQCXIN expression vector (Clontech, Paolo Alto, CA).

shRNA (GAG CAA GAT GTG GAC TTA G) spanning nucleotides 153–171 downstream of the transcription start site of MMP-1 mRNA have previously been shown to efficiently downregulate the expression of MMP-1 [24]. The scrambled shRNA, GAT TCA GGT GTA GAA CGA G [24], with no significant homology to any mammalian gene sequence was used as non-silencing control. Pairs of complementary oligonucleotides containing these sequences were synthesized (Mycrosynth, Balgach, Switzerland) and cloned into the pSIREN-Retro Q retroviral vector (Clontech). DNA sequences were verified by sequencing in both directions.

Retroviral particles containing the described constructs were produced in HEK293-T cells as described recently [25]. Briefly, HEK293-T cells were cultured in Advanced D-MEM medium (GIBCO) supplemented with 2% fetal calf serum and a culture additive containing 0.01 mM cholesterol (Sigma), 0.01 mM egg's lecithin (Serva Electrophoresis GmbH, Heidelberg, Germany) and 1× chemically defined lipid concentrate (GIBCO) (transfection medium). The cells were co-transfected using the calcium phosphate method with the following three plasmids: the retroviral expression or shRNA vector together with the two helper plasmids pVSV-G (Clontech), encoding the G-glycoprotein of the vesicular stomatitis virus, and pHit60 coding for the retroviral *gag* and *pol* genes (kindly provided by Dr. Christian Buchholz, Paul-Ehrlich-Institut, Langen, Germany). Fourteen hours after transfection the medium was

replaced with fresh transfection medium. The supernatant containing the respective recombinant retrovirus was collected 48 h after transfection, filtered through a 0.45 μm syringe filter, aliquoted and stored at −80 °C.

2.5. Generation of modified cell lines

HOS and 143-B OS cells were transduced with different viral supernatants for 2 h in the presence of 8 μg/ml polybrene (Sigma-Aldrich), and fresh cell culture medium was then added. HOS cells transduced with the empty vector (pQCXIN) and the vector overexpressing MMP-1 were selected in cell culture medium containing 1200 μg/ml G-418 (Invitrogen). 143-B cells transduced with a non-specific control shRNA (scrambled) or with the MMP-1 specific shRNA (153–171) were selected with 5 μg/ml Puromycin (Invitrogen). In all modified cell lines, MMP-1 protein expression was verified by Western blot analysis of cell supernatants.

In addition, all manipulated HOS and 143-B OS cell lines were transduced with the *lacZ* gene in order to facilitate and improve the identification and localization of OS cells in mouse tissues as described recently [25].

The manipulated cell lines were named HOS/LZ + EV (containing the empty pQCXIN vector), HOS/LZ + MMP-1 (overexpressing MMP-1), 143-B/LZ + scr (containing the unspecific, control shRNA) and 143-B/LZ + 153 (containing the MMP-1 specific shRNA sequence). Authentication of the cell lines was performed by multiplex PCR (Microsynth) using the PowerPlex®16HS system (Promega) and verified by comparison with the database at the German Collection of Microorganisms and Cell Cultures (DSMZ, Braunschweig, Germany).

2.6. Western blot

Supernatants from cultures of equal numbers of cells of the individual cell lines were collected 24 h after the last medium change and centrifuged for 10 min at 500 ×*g* to remove cell debris. 30 μl aliquots of collected cell supernatants were analyzed on Western blots as described recently [22]. Membranes were probed with a polyclonal rabbit antibody directed to MMP-1 (M4177, Sigma-Aldrich) at a dilution of 1:1000. Bound antibodies were detected with a horseradish peroxidase conjugated goat anti-rabbit antiserum from Santa Cruz Biotechnology (Santa Cruz, CA) at a dilution of 1:3000. The peroxidase-conjugated antibody was visualized by chemiluminescence with the Immobilon chemiluminescence substrate (Millipore, Billerica, MA) and the VersaDoc™ Imaging System (Bio-Rad Laboratories, Hercules, CA).

2.7. Adhesion assay

Wells of 96-well plates were coated for 1 h at room temperature (RT) with 100 μl/well collagen type I (Becton & Dickenson, Franklin Lakes, NJ) (1 μg/ml in water). They were then washed twice with 100 μl/well PBS, blocked with 100 μl/well 1% heat denatured BSA for 1 h at RT and washed once with 100 μl/well cell culture medium before cell seeding. Single cell suspensions were prepared with Accutase (Sigma-Aldrich). 5000 cells/well in 100 μl cell culture medium were plated and allowed to adhere to collagen type I for 15 min at 37 °C. Individual wells were washed once with 100 μl/well cell culture medium and with PBS and then fixed with 100 μl/well 10% formaldehyde for at least 15 min at RT. Cells were stained with DAPI and images were taken with a Nikon Eclipse E600 microscope (Nikon Corporation, Tokyo, Japan). The numbers of bound cells were quantified with the image processing program ImageJ [26]. The results are presented as the mean ± SEM of four independent experiments.

2.8. Soft-agar colony formation assay

The experiments were carried out in six-well cell culture plates containing 1.5 ml/well of 0.5% base agar in cell culture medium supplemented with PSA. Single cell suspensions (20,000 cells per well) of the individual cell lines prepared in 1.5 ml/well cell culture medium containing 0.35% agar and PSA (top agar) were seeded on the base agar and incubated in a humidified atmosphere of 95% air and 5% CO_2 at 37 °C. Twenty-four hours later the top agar was overlaid with 2 ml/well cell culture medium containing PSA. Cells were allowed to grow for 16 days and the medium was changed in 3 day intervals. Colonies were stained with 0.005% crystal violet. Images were taken with a Nikon Eclipse E600 microscope and the numbers of colonies larger than 200 μm^2 were counted with the image processing program ImageJ [26]. The results are presented as the mean ± SEM of four independent experiments.

2.9. In vivo experiments

Female 6–7 week old immunosuppressed SCID mice were purchased from Charles River Laboratories (Sulzfeld, Germany) and kept in individually ventilated cages (IVC). Housing and experimental protocols were in accordance with the Swiss Animal Protection Law and in compliance with the regulations of the Veterinäramt, Kanton Zurich. All manipulations were done under sterile conditions in a laminar flow hood.

All cell lines were grown to subconfluency, detached with Trypsin/EDTA/PBS and prepared as single cell suspension in PBS/0.05% EDTA at a density of 5×10^7 cells/ml. Ten microliters of the cell suspension containing 5×10^5 cells were orthotopically injected into the medullar cavity of the left proximal tibia of the mice. The injection was performed with a Hamilton syringe through an opening of the tibia plateau pre-made with a 26-gauge needle. Tumor growth and osteolysis were monitored by X-ray analysis once a week with the Faxitron® MX-20 Specimen Radiography System (Faxitron X-Ray LLC, Lincolnshire, IL). The tumor volume (V) was calculated from the measurement of two perpendicular diameters using a caliper rule, according to the following formula: $V = 0.5 \times L \times (S)^2$ (L and S are, respectively, the largest and smallest perpendicular tumor diameters), Tumor volume = Volume of injected leg − Volume of control leg. Organs and legs of the mice were prepared at sacrifice and stained with 5-bromo-4-chloro-3-indolyl-β-D-galactoside (X-gal) as described recently [25]. For quantification of macro- and micrometastases, images of the surface of one lung lobe of individual mice were taken under a Nikon Eclipse E600 microscope with a Kappa PS 20 C digital camera (Kappa optronics GmbH, Gleichen, Germany) and imported as TIF files into Power Point© software. Indigo-blue stained foci on lung surfaces with a diameter >0.1 mm were defined as macrometastases and foci with a diameter <0.1 mm as micrometastases. The results are presented as the mean ± SEM number respective metastases counted in at least five mice injected with indicated cell lines.

2.10. Statistical analyses

Experimental data sets were analyzed with the two-tailed Student's *t* test using the GraphPad Prism5 software (La Jolla, CA). *P* values <0.05 were considered as significant.

3. Results

3.1. MMP-1 expression in primary OS cells and OS cell lines

The expression of MMP-1 at the transcript level was analyzed by real-time PCR in primary human OS cells and compared to the expression in normal human bone cells. In the group of primary

cells from patients who are dead (Ø 23 months after diagnosis), we detected in six out of nine samples a >2 fold higher MMP-1 expression than in NHB cells (Table 1). In the second group of primary cells from patients still alive (Ø 42 months after diagnosis), only two of nine samples showed a >2 fold higher MMP-1 expression than in NHB cells (Table 1).

MMP-1 expression was further analyzed in the established HOS human OS cell line [27] and two sublines thereof, the chemically mutated MNNG/HOS cells and the highly metastatic Ki-ras transformed 143-B cells [28,29]. MMP-1 was found upregulated at the mRNA and at the protein levels in 143-B compared to HOS and MNNG/HOS cells (Fig. 1A,B). In addition to MMP-1, MMP-8 and MMP-13 are secreted proteinases, which are able to cleave native fibrillar collagens of types I, II, III, V and IX [9]. Therefore, we also investigated the expression and a potential regulation of MMP-8 and MMP-13 in these cell lines. MMP-8 transcripts were nondetectable in all three OS cell lines and the levels of MMP-13 encoding mRNA were comparable in the parental HOS cells and in the highly metastatic 143-B cells (Fig. 1A).

3.2. MMP-1 promotes cell adhesion and anchorage independent colony formation in soft agar

The functional relevance of MMP-1 in OS in vitro and in vivo was analyzed in *lacZ*-tagged HOS cells overexpressing MMP-1 (HOS/LZ + MMP-1) and in *lacZ*-tagged 143-B cells with shRNA down-regulated MMP-1 expression (143-B/LZ + 153). MMP-1 protein expression in the generated cell lines was verified by Western blotting of cell supernatants and compared with the corresponding HOS/LZ + EV (containing the empty vector) and 143-B/LZ + scr (expressing non-specific shRNA) control cells. 143-B/LZ + 153 cells showed effective suppression of MMP-1 expression when compared to the 143-B/LZ + scr control cells (Fig. 1C). MMP-1 was nondetectable in supernatants of HOS/LZ + EV cells, whereas in HOS/LZ + MMP-1 cells the protein was detected at the expected molecular weight of 52 kDa (Fig. 1C).

Potential effects of up- or downregulated MMP-1 expression were first analyzed in vitro in a cell adhesion assay with collagen type I as substrate. Downregulation of MMP-1 expression in 143-B/LZ + 153 cells reduced the percentage of adhering cells significantly (P value < 0.05) by more than 40% when compared to control 143-B/LZ + scr cells (Fig. 2A, B). The number of adhering HOS/LZ + MMP-1 cells, on the other hand, was more than two times higher than that of HOS/LZ + EV control cells (Fig. 2A,B).

Anchorage independent growth, another important in vitro indicator of malignant properties of cell lines, was investigated in a soft agar assay. Downregulation of MMP-1 in 143-B/LZ + 153 cells resulted in reduced anchorage independent growth. The number of large colonies (area > 200 μm^2) was reduced by more than 60% compared to that of 143-B/LZ + scr cells (Fig. 3A,B). In contrast, in cultures of HOS/LZ + MMP-1 cells, the number of large colonies was more than 6-fold higher than in cultures of HOS/LZ + EV control (Fig. 3A,B).

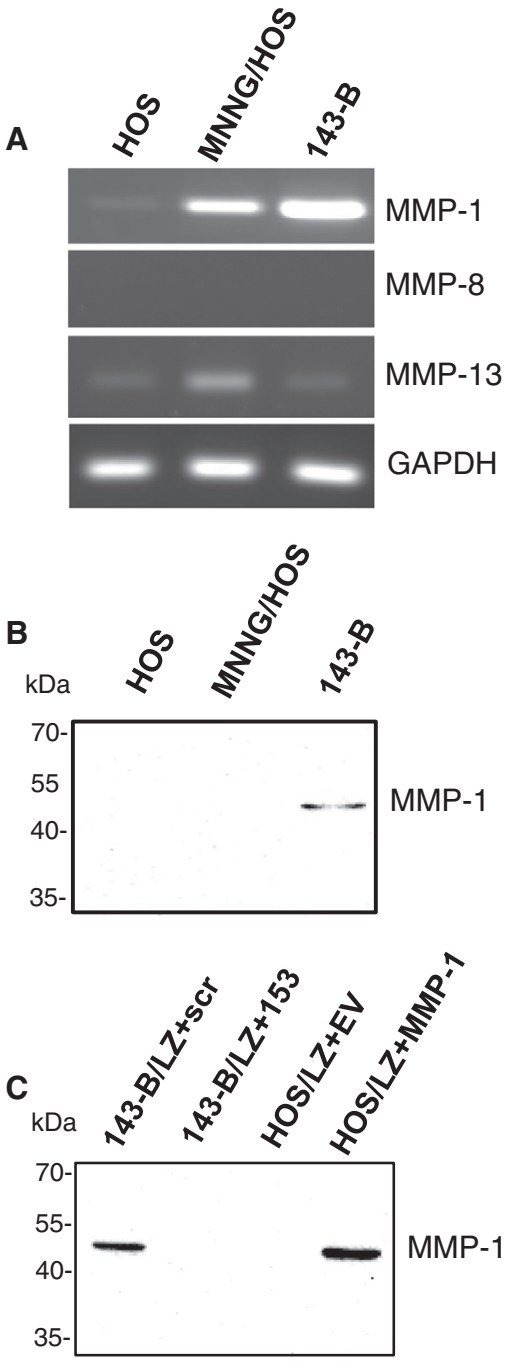

Fig. 1. MMP-1 expression in human OS cells. (A) Expression of MMP-1, MMP-8, MMP-13 and GAPDH encoding mRNAs in HOS, MNNG/HOS and 143-B cells. (B) MMP-1 protein in supernatants of HOS, MNNG/HOS and 143-B cells and (C) of MMP-1 expression-manipulated HOS/LZ and 143-B/LZ cells. mRNA levels in (A) were analyzed by semi-quantitative RT-PCR, and PCR products were separated by electrophoresis in 1.2% agarose gels. MMP-1 in culture medium (B) and (C) was analyzed on Western blots.

Table 1
Real time PCR for MMP-1 expression in primary osteosarcoma cells and normal human bone cells.

MMP-1 expression	Dead patients	Alive patients
>2 fold of NHB	6	2
≤2 fold of NHB	3	7

NHB: normal human bone cells.

3.3. MMP-1 promotes intratibial primary tumor growth and lung metastasis

The in vitro characterization of malignant properties of the OS cell lines with manipulated MMP-1 expression suggested tumor and metastasis promoting function(s) of MMP-1 in vivo. When the manipulated cell lines were orthotopically injected into the tibiae of SCID mice, no differences in frequency of primary tumor formation were observed. However, intratibial injection of 143-B/LZ + scr control

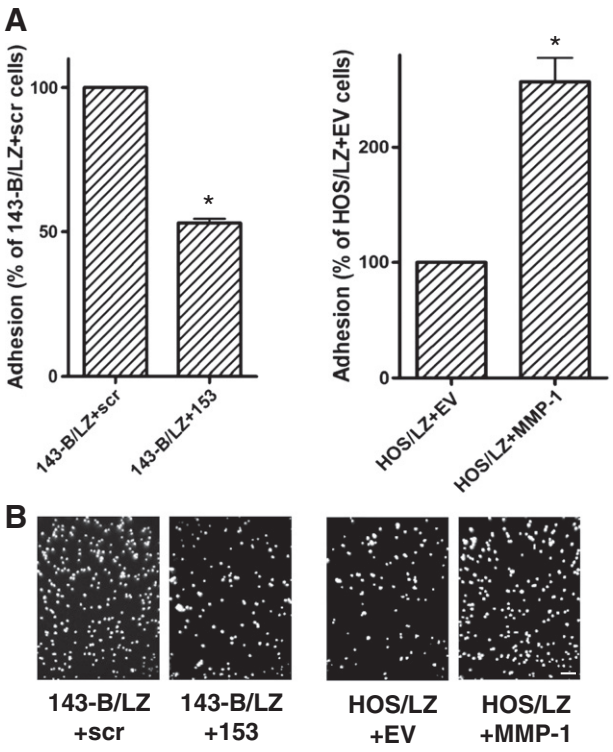

Fig. 2. MMP-1 enhances adhesion of 143-B/LZ and HOS/LZ OS cells to collagen type I. (A) Adhesion of indicated 143-B/LZ (left panel) and HOS/LZ (right panel) derived cells to collagen type I. The number of adhering 143-B/LZ + scr (left panel) or HOS/LZ + EV (right panel) control cells was set to 100%. The results are the mean ± SEM of four independent experiments. * P value < 0.05. (B) Representative images of cell adhesion experiments of indicated cell lines. Bar: 50 μm.

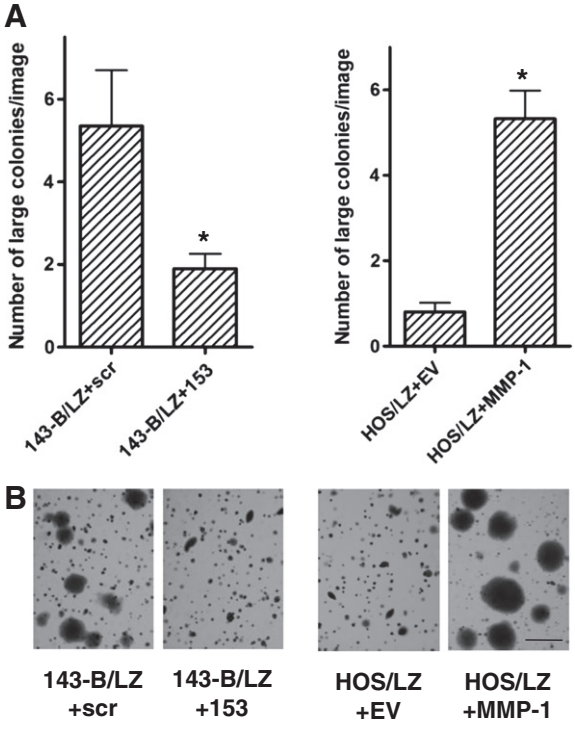

Fig. 3. MMP-1 enhances anchorage-independent growth of 143-B/LZ and HOS/LZ OS cells. (A) Anchorage independent growth of indicated 143-B/LZ (left panel) and HOS/LZ (right panel) derived cells. The results are the mean ± SEM of four independent experiments. * P value < 0.05. (B) Representative images of anchorage independent growth of indicated cell lines. Bar: 500 μm.

cells resulted in radiologically detectable osteolysis already on day 9 after tumor cell injection, when none of the animals injected with 143-B/LZ + 153 cells showed any signs of intratibial primary tumors (not shown). Twenty days after tumor cell injection the mice of both groups were sacrificed. The mice of the 143-B/LZ + scr control group presented primary tumors with a mean volume of 247 ± 48 mm^3 (Fig. 4B) and extensive osteolytic destruction of the tibia (Fig. 4A, left panel). In contrast, the group of mice injected with 143-B/LZ + 153 cells developed much smaller primary tumors with a mean volume of 31 ± 12 mm^3 (P value < 0.05) (Fig. 4B), and osteolysis was much less extensive compared with the mice injected with the 143-B/LZ + scr control cells (Fig. 4A).

Lung metastasis formation was also analyzed after sacrificing the mice on day 20. Micrometastases (diameter < 0.1 mm) were found on the lungs of the 143-B/LZ + scr group at a mean number of 330 ± 117 micrometastases per lung, which was significantly (P value < 0.05) higher than that (45 ± 14.7) detected in the group injected with 143-B/LZ + 153 cells (Fig. 5A,B). The number of macrometastases (diameter > 0.1 mm) was also significantly (P value < 0.05) higher in

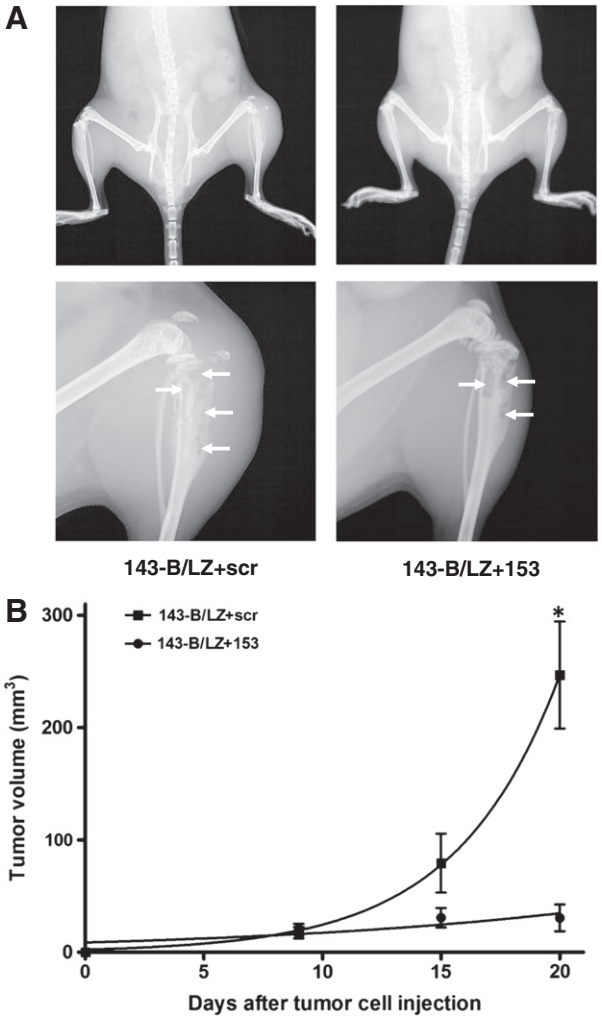

Fig. 4. shRNA-mediated MMP-1 knockdown in 143-B/LZ cells reduces intratibial primary tumor growth. (A) Representative X-ray images of legs from mice injected with 143-B/LZ + scr cells (left panels) or 143-B/LZ + 153 cells (right panels) 20 days after tumor cell injection showing the hindlimbs (top panels) and the leg injected with tumor cells at a higher magnification (bottom panels). Arrows indicate osteolytic lesion areas. (B) Primary tumor growth over time in mice intratibially injected with 143-B/LZ + scr cells (■) (five mice) or with 143-B/LZ + 153 cells (●) (eight mice). Data are the mean ± SEM calculated tumor volumes at indicated time points. * P value < 0.05.

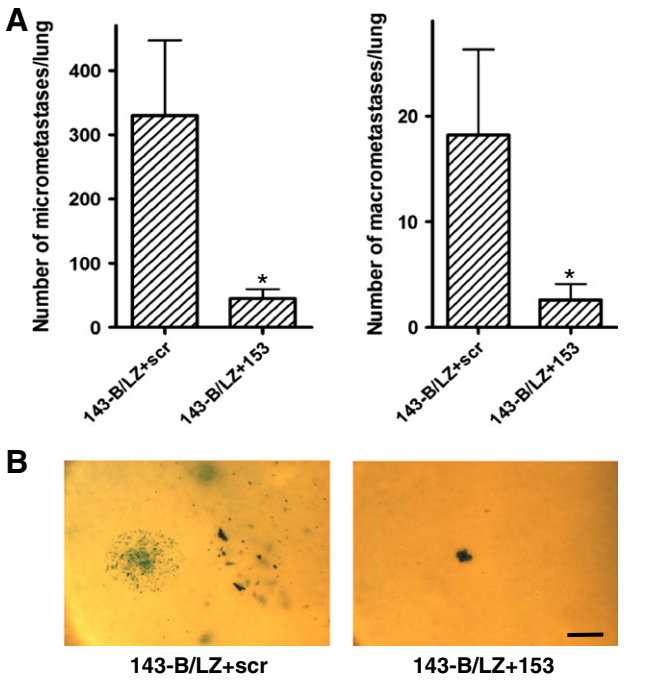

Fig. 5. shRNA-mediated knockdown of MMP-1 in 143-B/LZ OS cells reduces lung metastases formation. (A) Number of lung micrometastases (left panel) and macrometastases (right panel) in mice injected with 143-B/LZ + scr (five mice) or 143-B/LZ + 153 (eight mice) cells. Data are shown as the mean ± SEM of at least 5 animals. * *P* value < 0.05. (B) Representative images show metastases on X-Gal stained lungs of mice injected with 143-B/LZ + scr cells or with 143-B/LZ + 153 cells 20 days after tumor cell injection. Bar: 50 μm.

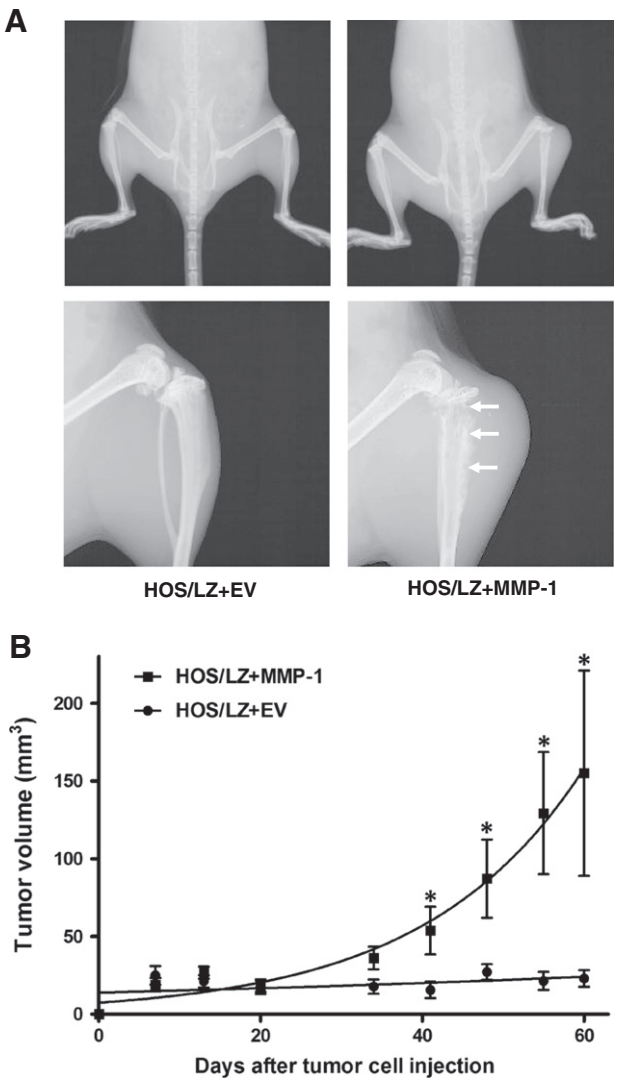

Fig. 6. MMP-1 overexpression of HOS/LZ cells induces intratibial primary tumor growth. (A) Representative X-ray images of legs from mice injected with HOS/LZ + EV cells (left panels) or HOS/LZ + MMP-1 cells (right panels) 60 days after tumor cell injection showing the hindlimbs (top panels) and the leg injected with tumor cells at a higher magnification (bottom panels). Arrows indicate osteolytic lesion areas. (B) Primary tumor growth over time in mice intratibially injected with HOS/LZ + EV cells (●) (eight mice) or HOS/LZ + MMP-1 cells (■) (seven mice). Data are the mean ± SEM calculated tumor volume at indicated time points. * *P* value < 0.05.

the group injected with 143-B/LZ + scr cells group (18.2 ± 8.1) than in the group injected with 143-B/LZ + 153 cells (2.6 ± 1.5) (Fig. 5A,B).

These results prompted us to investigate the properties of HOS/LZ + MMP-1 cells in vivo for tumor and metastasis formation, although it has been shown previously that non-manipulated HOS cells orthotopically injected into nude mice formed neither primary tumors nor metastases [30]. This observation was confirmed in the present study. The group of mice injected with HOS/LZ + EV control cells developed no radiologically detectable primary tumors (Fig. 6A, left panel). In contrast, injection of HOS/LZ + MMP-1 cells resulted in radiologically detectable primary tumors after 6 weeks (not shown) and X-ray images showed massive osteolytic destruction of the tibiae at the end of the study on day 60 (Fig. 6A, right panel). Tumor growth in the HOS/LZ + MMP-1 group was measurable 35 days after cell injection and the average tumor volume was 155 ± 66 mm^3 at the end of the study (Fig. 6B). On day 41 and later the mean calculated volume of the tumors was significantly (*P* value < 0.05) larger than that of the HOS/LZ + EV-injected mice, which showed no measurable difference between the mean calculated volume of both legs (Fig. 6B). Sixty days after tumor cell injection the experiment was terminated and the animals of both groups were therefore sacrificed. Mice injected with HOS/LZ + MMP-1 cells had a mean number of 249 ± 94.5 micrometastases (diameter < 0.1 mm) per lung (Fig. 7A,B) but no macrometastases (diameter > 0.1 mm). In contrast and as expected, the lungs of HOS/LZ + EV control mice with no detectable primary tumors were free of metastases (Fig. 7A,B).

4. Discussion

Several members of the large family of MMPs are known to be involved in the complex processes of metastasis including cell proliferation, tissue remodeling, cell migration and invasion. However, only a small group of proteases including MMP-1, -8, -13, and -14 is able to cleave native fibrillar collagen type I, the predominant ECM protein in bone. Proteolysis of the bone ECM is a prerequisite for primary tumor growth and metastasis formation in OS. Recently, important markers for metastatic spreading of breast cancer cells to the lung and to the bone were identified [15,31,32]. Interestingly, MMP-1 belongs to both marker groups mediating metastasis in different organs such as bone and lung.

In the present study, the role of MMP-1 in OS tumor growth and metastasis was investigated in vitro and in vivo. In normal human bone cells, MMP-1 mRNA expression was low or non-detectable by RT-PCR. In contrast, robust MMP-1 expression was detected in primary OS cells and to an even higher level in the well-established highly metastatic human 143-B OS cell line. Also Kimura et al. found a strong MMP-1 expression in 143-B cells when they compared gene expression profiles of 143-B cells with those of the related MNNG/HOS cells [33]. The observed co-expression of MMP1 and MMP-13 in the absence of MMP-8 (Fig. 1) suggested a synergistic function, which was also reported for giant cell tumor of bone, a primary osteolytic bone tumor [16]. However, the highly metastatic 143-B OS tumor

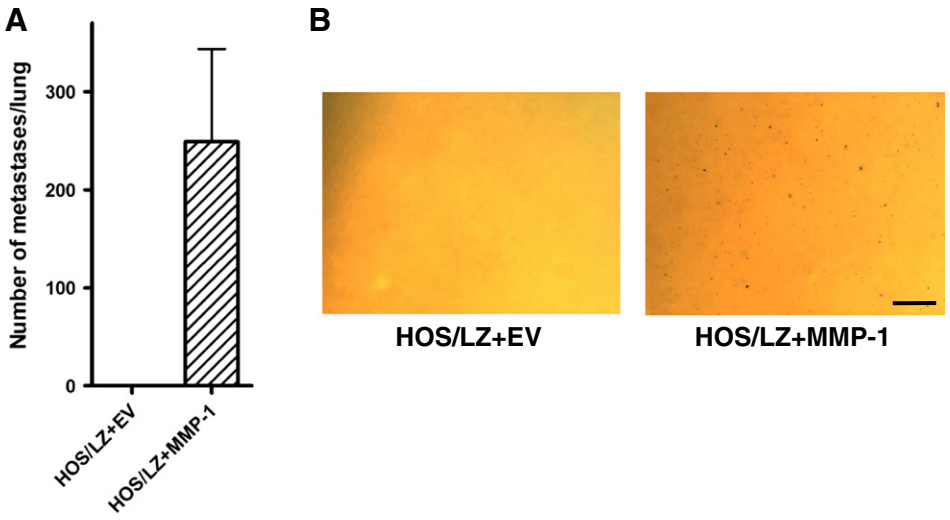

Fig. 7. MMP-1 overexpression in HOS/LZ cells mediates lung metastases formation. (A) Number of lung metastases in mice injected with HOS/LZ + EV (eight mice) or HOS/LZ + MMP-1 (seven mice) cells. Data are the mean ± SEM of at least 7 animals. (B) Representative images of X-Gal stained lungs from mice injected with HOS/LZ + EV cells or HOS/LZ + MMP-1 cells 60 days after tumor cell injection. Bar: 50 μm.

cells express both MMP-1 and MMP-13 whereas in giant cell tumors both proteases are produced by surrounding stromal cells [16]. Remarkably, both cell types contribute to the formation of primary tumors through the degradation of type I collagen.

Cell adhesion to collagen type I and anchorage independent colony formation assays were performed to characterize in vitro the malignant potential of the OS cell lines with manipulated MMP-1 expression. Increased adhesion of tumor cells to collagen type I as found for the OS cells with high MMP-1 expression may reduce cell mobility, but it also brings the tumor cells in a more stable contact with the collagen of the ECM and the blood vessels for destruction. Both processes are necessary for the escape of the tumor cells from the primary tumor region. Increased soft agar colony formation of the analyzed OS cell lines was observed in an MMP-1 dependent manner (Fig. 3A,B). Proteolytic activation by MMP-1 of cell surface receptors or MMP1 dependent processing of ECM associated growth factors required for anchorage independent growth may be involved in colony forming processes. These results are in line with the recently reported MMP-1 enhanced invasion of collagen type I matrices by OS cells [33,34], or with MMP-1 mediated collagen matrix degradation by breast cancer cells [35,36].

An earlier study reported that orthotopic injection of HOS cells into the tibia of athymic mice revealed neither primary tumors nor metastases [30]. This was confirmed in the present study with our *lacZ*-transduced control cells (HOS/LZ + EV). In contrast, intratibial injection of HOS cells overexpressing only MMP-1 (HOS/LZ + MMP-1) resulted in the growth of large primary tumors with remarkable osteolysis and metastasis to the lung within 60 days. The destruction of the bone ECM around the primary tumor is one of the first critical events for primary tumor growth and metastatic spreading to distant organs, in OS mainly to the lung [37]. Apparently, the low levels of endogenously expressed MMP-1 in the parental HOS cells are insufficient to induce tumor growth and metastasis. However, when MMP-1 expression was up-regulated by stable transduction with MMP-1 encoding cDNA, HOS cells became tumorigenic, which strongly indicated a critical role of this protease in OS primary tumor formation.

This was further supported by the observation of delayed development of primary tumors derived from the highly tumorigenic 143-B cells after shRNA mediated downregulation of MMP-1. However, 143-B/LZ + scr cell-derived primary tumors were still growing faster and became detectable 20 days earlier than those derived from HOS/LZ + MMP1 cells despite the fact that both cell lines expressed comparable levels of MMP-1 protein in vitro. MMP-1 is likely acting in concert with other proteases, secreted either by tumor cells or the surrounding stroma cells that facilitate primary tumor formation in the bone. One of these proteases, cathepsin K, has been described recently as a marker for OS metastasis [22]. Primary tumor formation may also be supported by inhibitors of osteoblast activity or activators of osteoclast activity, resulting in an imbalance between bone formation and bone resorption [38]. Nemeth et al. [39] postulated that metastatic prostate cancer cells, similar to osteoblasts, enhance osteoclastic bone resorption. Activation or inhibition of osteoblasts or osteoclasts can be mediated by direct contact of the tumor cells with the surrounding stroma cells or by soluble factors [40].

Micrometastases developed in the lungs of mice after intratibial injection of HOS cells overexpressing MMP-1. Conversely, 143-B cells with MMP-1 expression downregulated by shRNA generated fewer lung micro- and macrometastases compared to control cells, similar to the results recently published for non *lac*Z-tagged 143-B cells [34]. Our results support the hypothesis that MMP-1 is not only involved in primary tumor growth, but also assists the formation of lung metastases in our OS models. Interestingly, the metastases found in mice injected with 143-B cells with downregulated MMP-1 expression were still larger than those found in animals injected with HOS cells overexpressing MMP-1, even though the time period until analysis was 3-times longer in the experiment with the MMP1-transduced HOS cells (60 instead of 20 days). This may be attributable to the slower primary tumor growth of the HOS/LZ + MMP-1 compared to the 143B/LZ cells and, consequently, delayed metastatic spread. However, it is also conceivable that factors required for the outgrowth of micrometastases in the lung are lacking. Collectively, these data indicate that the incidence and progression of HOS lung metastases are dependent on MMP-1 expression and also regulated by other factors differentially expressed in the HOS and 143-B cells, which remain to be identified. In conclusion, the results obtained with the mouse models presented here suggest that in OS, MMP-1 is an important factor involved in primary tumor growth and lung metastasis.

Competing interests

None of the authors declares any competing interests.

Acknowledgements

The authors thank Dr Emanuel E. Strehler (Department of Biochemistry and Molecular Biology, Mayo Clinic College of Medicine, Rochester) for critical reading of this manuscript. This study was supported by the Swiss National Science Foundation SNF, the Schweizerischer Verein Balgrist, the University of Zurich, the Krebsliga Zurich, a grant from the Walter L. and Johanna Wolf Foundation, Zurich, Switzerland, and the HSM program for Muskuloskeletal Oncology of the Kanton Zurich.

References

[1] B. Fuchs, D.J. Pritchard, Etiology of osteosarcoma, Clin. Orthop. Rel. Res. 397 (2002) 40–52.
[2] C. Khanna, K. Hunter, Modeling metastasis in vivo, Carcinogenesis 26 (2005) 513–523.
[3] D.X. Nguyen, P.D. Bos, J. Massagué, Metastasis: from dissemination to organ-specific colonization, Nat. Rev. Cancer 9 (2009) 274–284.
[4] E. Skrzydlewska, M. Sulkowska, M. Koda, S. Sulkowski, Proteolytic–antiproteolytic balance and its regulation in carcinogenesis, World J. Gastroenterol. 11 (2005) 1251–1266.
[5] S.A. Brooks, H.J. Lomax-Browne, T.M. Carter, C.E. Kinch, D.M. Hall, Molecular interactions in cancer cell metastasis, Acta Histochem. 112 (2010) 3–25.
[6] M.D. Sternlicht, Z. Werb, How matrix metalloproteinases regulate cell behaviour, Annu. Rev. Cell Dev. Biol. 17 (2001) 463–516.
[7] M. Egeblad, Z. Werb, New functions for the matrix metalloproteinases in cancer progression, Nat. Rev. Cancer 2 (2002) 161–174.
[8] E.I. Deryugina, J.P. Quigley, Matrix metalloproteinases and tumor metastasis, Cancer Metastasis Rev. 25 (2006) 9–34.
[9] R. Ala-aho, V.-M. Kähäri, Collagenases in cancer, Biochimie 87 (2005) 273–286.
[10] C.E. Brinckerhoff, J.L. Rutter, U. Benbow, Interstitial collagenases as markers of tumor progression, Clin. Cancer Res. 6 (2000) 4823–4830.
[11] G.I. Murray, M.E. Duncan, P. O'Neil, J.A. McKay, W.T. Melvin, J.E. Fothergill, Matrix metalloproteinase-1 is associated with poor prognosis in oesophageal cancer, J. Pathol. 185 (1998) 256–261.
[12] G.I. Murray, M.E. Duncan, P. O'Neil, W.T. Melvin, J.E. Fothergill, Matrix metalloproteinase-1 is associated with poor prognosis in colorectal cancer, Nat. Med. 2 (1996) 461–462.
[13] J. Nikkola, P. Vihinen, T. Vlaykova, M. Hahka-Kemppinen, V.-M. Kähäri, S. Pyrhönen, High expression levels of collagenase-1 (MMP-1) and stromelysin-1 (MMP-3) correlate with shorter disease free survival in human metastatic melanoma, Int. J. Cancer 97 (2002) 432–438.
[14] A. Kawashima, Y. Okada, I. Nakanishi, Y. Ueda, K. Iwata, A. Roessner, Immunolocalization of matrix metalloproteinases and tissue inhibitors of metalloproteinases in human chondrosarcomas, Gen. Diagn. Pathol. 142 (1997) 129–137.
[15] Y. Kang, P.M. Siegel, W. Shu, M. Drobnjak, S.M. Kekkonen, C. Cordón-Cardo, T.A. Guise, J. Massagué, A multigenic program mediating breast cancer metastasis to bone, Cancer Cell 3 (2003) 537–549.
[16] R.W. Cowan, I.W.Y. Mak, N. Colterjohn, G. Singh, M. Ghert, Collagenase expression and activity in the stromal cells from giant cell tumour of bone, Bone 44 (2009) 865–871.
[17] C. Ferrari, M.S. Benassi, F. Ponticelli, G. Gamberi, P. Ragazzini, L. Pazzaglia, A. Balladelli, F. Bertoni, P. Picci, Role of MMP-9 and its tissue inhibitor TIMP-1 in human osteosarcoma: findings in 42 patients followed for 1–16 years, Acta Orthop. Scand. 75 (2004) 487–491.
[18] K. Bjørnland, K. Flatmark, S. Pettersen, A.O. Aaasen, O. Fodstad, G.M. Maelandsmo, Matrix metalloproteinases participate in osteosarcoma invasion, J. Surg. Res. 127 (2005) 151–156.
[19] M. Uchibori, Y. Nishida, T. Nagasaka, Y. Yamada, K. Nakanishi, N. Ishiguro, Increased expression of membrane-type matrix metalloproteinase-1 is correlated with poor prognosis in patients with osteosarcoma, Int. J. Oncol. 28 (2006) 33–42.
[20] J.T. Korpi, J. Hagström, N. Lehtonen, J. Parkkinen, T. Sorsa, T. Salo, M. Laitinen, Expression of matrix metalloproteinases-2, -8, -13, -26, and tissue inhibitors of metalloproteinase-1 in human osteosarcoma, Surg. Oncol. 20 (2011) e18–e22.
[21] D.K. Walters, R. Muff, B. Langsam, P. Gruber, W. Born, B. Fuchs, Taurolidine: a novel anti-neoplastic agent induces apoptosis of osteosarcoma cell lines, Invest. New Drugs 25 (2007) 305–312.
[22] K. Husmann, R. Muff, M.E. Bolander, G. Sarkar, W. Born, B. Fuchs, Cathepsins and osteosarcoma: expression analysis identifies cathepsin K as an indicator of metastasis, Mol. Carcinog. 47 (2008) 66–73.
[23] K.J. Livak, T.D. Schmittgen, Analysis of relative gene expression data using real-time quantitative PCR and the 2(-Delta Delta C(T)) method, Methods 25 (2001) 402–408.
[24] J. Yuan, C.M. Dutton, S.P. Scully, RNAi mediated MMP-1 silencing inhibits human chondrosarcoma invasion, J. Orthop. Res. 23 (2005) 1467–1474.
[25] M.J.E. Arlt, I.J. Banke, D.K. Walters, G.J. Puskas, P. Steinmann, R. Muff, W. Born, B. Fuchs, LacZ transgene expression in the subcutaneous Dunn/LM8 osteosarcoma mouse model allows for the identification of micrometastasis, J. Orthop. Res. 29 (2011) 938–946.
[26] M.D. Abramoff, P.J. Magelhaes, S.J. Ram, Image processing with Image J, Biophotonics Int. 11 (2004) 36–42.
[27] R.M. McAllister, M.B. Gardner, A.E. Greene, C. Bradt, W.W. Nichols, B.H. Landing, Cultivation in vitro of cells derived from a human osteosarcoma, Cancer 27 (1971) 397–402.
[28] J.S. Rhim, D.L. Putman, P. Arnstein, R.J. Huebner, R.M. McAllister, Characterization of human cells transformed in vitro by N-methyl-N′-nitro-N-nitrosoguanidine, Int. J. Cancer 19 (1977) 505–510.
[29] O. Berlin, D. Samid, R. Donthineni-Rao, W. Akeson, D. Amiel, V.L. Woods Jr., Development of a novel spontaneous metastasis model of human osteosarcoma transplanted orthotopically into bone of athymic mice, Cancer Res. 53 (1993) 4890–4895.
[30] H.H. Luu, Q. Kang, J.K. Park, W. Si, Q. Luo, W. Jiang, H. Yin, A.G. Montag, M.A. Simon, T.D. Peabody, R.C. Haydon, C.W. Rinker-Schaeffer, T.C. He, An orthotopic model of human osteosarcoma growth and spontaneous pulmonary metastasis, Clin. Exp. Metastasis 22 (2005) 319–329.
[31] A.J. Minn, G.P. Gupta, P.M. Siegel, P.D. Bos, W. Shu, D.D. Giri, A. Viale, A.B. Olshen, W.L. Gerald, J. Massagué, Genes that mediate breast cancer metastasis to lung, Nature 436 (2005) 518–524.
[32] S.A. Eltarhouny, W.H. Elsawy, R. Radpour, S. Hahn, W. Holzgreve, X.Y. Zhong, Genes controlling spread of breast cancer to lung "gang of 4", Exp. Oncol. 30 (2008) 91–95.
[33] R. Kimura, C. Ishikawa, T. Rokkaku, R. Janknecht, N. Mori, Phosphorylated c-Jun and Fra-1 induce matrix metalloproteinase-1 and thereby regulate invasion activity of 143B osteosarcoma cells, Biochim. Biophys. Acta 1813 (2011) 1543–1553.
[34] M.U. Jawad, N. Garamszegi, S.P. Garamszegi, M. Correa-Medina, J.A. Diez, R. Wen, S.P. Scully, Matrix metalloproteinase 1: role in sarcoma biology, PLoS One 5 (2010) e14250.
[35] C.A. Wyatt, J.C. Geoghegan, C.E. Brinckerhoff, Short hairpin RNA-mediated inhibition of matrix metalloproteinase-1 in MDA-231 cells: effects on matrix destruction and tumor growth, Cancer Res. 65 (2005) 11101–11108.
[36] S.M. Eck, P.J. Hoopes, B.L. Petrella, C.I. Coon, C.E. Brinckerhoff, Matrix metalloproteinase-1 promotes breast cancer angiogenesis and osteolysis in a novel in vivo model, Breast Cancer Res. Treat. 116 (2009) 79–90.
[37] R. Gorlick, C. Khanna, Osteosarcoma, J. Bone Min. Res. 25 (2010) 683–691.
[38] J.T. Buijs, G. van der Pluijm, Osteotropic cancers: from primary tumor to bone, Cancer Lett. 273 (2009) 177–193.
[39] J.A. Nemeth, R. Yousif, M. Herzog, M. Che, J. Upadhyay, B. Shekarriz, S. Bhagat, C. Mullins, R. Fridman, M.L. Cher, Matrix metalloproteinase activity, bone matrix turnover, and tumor cell proliferation in prostate cancer bone metastasis, J. Natl. Cancer Inst. 94 (2002) 17–25.
[40] N. Giuliani, V. Rizzoli, Myeloma cells and bone marrow osteoblast interactions: role in the development of osteolytic lesions in multiple myeloma, Leuk. Lymphoma 48 (2007) 2323–2329.